Target residues from the interaction of copper with 35 MeV/nucleon ^{12}C ions

S. Y. Cho, Y. H. Chung,* and N. T. Porile

Department of Chemistry, Purdue University, West Lafayette, Indiana 47907

D. J. Morrissey

National Superconducting Cyclotron Laboratory, Michigan State University, East Lansing, Michigan 48824

(Received 8 September 1987)

Target residues from the interaction of copper with 35 MeV/nucleon ^{12}C ions have been studied by off-line γ-ray spectroscopy. Cross sections, average forward ranges, and forward-to-backward ratios were measured for 35 products. The data were used to obtain the isobaric yield distribution, the mass yield distribution, and the longitudinal momentum transfer. The results are compared with other studies of the interaction of copper with intermediate-energy projectiles and with various models.

I. INTRODUCTION

Nuclear reactions induced by intermediate-energy heavy ions have attracted considerable interest in recent years because of the change in the dynamics of the interaction that occurs at these energies. Low-energy ($E \leq 10$ MeV/nucleon) reactions are dominated by mean field dynamics and involve complete fusion and deep inelastic processes. On the other hand, high-energy ($E \gtrsim 200$ MeV/nucleon) reactions involve the dynamics of nucleon-nucleon collisions, and can be described by participant-spectator models. While the low- and high-energy regimes have been studied extensively, the regime of intermediate energies has become the subject of experimental study only in recent years, with the advent of accelerators designed for these energies.

The measurement of the cross sections and recoil properties of target fragmentation products has been one of the techniques that has been widely used to study the mechanisms of reactions induced by heavy ions. Depending on the details of the experiment, one can determine the isobaric-yield and mass yield distributions, the longitudinal momentum transfer, the angular distributions, and the energy spectra of the products. These techniques have been extensively applied to a study of the reactions of copper with heavy ions. Cumming and collaborators have measured the cross sections and thick-target recoil ranges of products of the interaction of copper with relativistic heavy ions.[1-5] Additional measurements at relativistic energies have been reported by Hicks et al.[6] and by Cole and Porile.[7,8] Similar experiments have been performed with 86 MeV/nucleon ^{12}C ions.[9-11] The longitudinal momentum transfer has also been measured for reactions induced by 22 and 84 MeV/nucleon ^{12}C ions.[12] The results of these studies show that factorization and limiting fragmentation are generally applicable at relativistic energies. The longitudinal momentum transfer, expressed as a fraction of the projectile momentum, varies inversely with projectile energy, and approaches unity at 22 MeV/nucleon. The mass yield curve obtained at 86 MeV/nucleon drops off somewhat more steeply than those obtained at relativistic energies, indicating that the mean excitation energy transfer scales with the total projectile kinetic energy in this regime.

We report here the results of a study of the interaction of copper with 35 MeV/nucleon ^{12}C ions, an energy significantly lower than those for which both yield and recoil measurements have been reported previously. The experiment involved the assay by off-line γ-ray spectrometry of target and catcher foils irradiated in a thick target–thick catcher configuration. Thus, the experiment permits a determination of the isobaric-yield and mass yield distributions and the mean longitudinal momentum transfer associated with the formation of specific products. Comparison with similar results obtained at higher energies permits us to trace the evolution of the dynamics down to projectile energies comparable to the Fermi energy.

II. EXPERIMENT

The experiment was performed at the K500 cyclotron of the National Superconducting Cyclotron Laboratory (NSCL) of Michigan State University. The target stack consisted of a 99.999% pure copper foil, 20.7 mg/cm^2 thick, surrounded by 10.1 mg/cm^2 thick Mylar catcher foils. Additional Mylar foils served as activation blanks, and the stack was surrounded by Mylar foils, which served to guard the other foils from possible external sources of radioactive products.

The target stack was mounted in an evacuated chamber terminated with a Faraday cup, and irradiated with 35 MeV/nucleon ^{12}C ions. The energy at the center of the target was reduced to 33.4 MeV/nucleon (~ 400 MeV) owing to the energy loss in Mylar and copper.[13] The beam was focused to a diameter of 3–5 mm. Two irradiations were performed, 30 min and 3.5 h in duration, with intensities of 10–30 e nA. For the short run, the fluence was read off a current integrator at periodic intervals in order to make it possible to correct short-lived activities for any significant variations in

beam intensity. The corrections for this effect were less than 1% in all cases.

Following bombardment, the various foils were assayed with calibrated Ge(Li) and intrinsic Ge γ-ray spectrometers. The samples from the short irradiation were assayed at NSCL for approximately 24 h commencing 20–40 min after the end of bombardment. Those from the longer irradiation were transported to Purdue University, where assay commenced 1 d following the irradiation and continued for a period of several months. The distance between the samples and the detector face during assay, typically 5–10 cm, was sufficiently large to ensure that the analyzer dead time was less than 5%. The intensities of 114 γ rays were determined with the code SAMPO,[14] and decay curves were analyzed with the CLSQ code.[15] Nuclidic assignments were made on the basis of energy, half-life, and concordance with other γ rays emitted by a presumed nuclide.[16]

III. RESULTS

A. Cross sections

Cross sections were determined for 35 nuclides; they are listed in Table I, where each entry is the weighted average of as many as nine separate determinations (two runs, several γ rays). The tabulated uncertainties are the larger of the standard deviation in the mean value and the estimated uncertainty of the individual determinations. The latter are based on the propagation of the errors in the SAMPO and CLSQ fits and also include a 5% uncertainty in detector efficiencies. In addition, a 5% uncertainty has been folded into the overall uncertainty of cross sections based on a single determination of a single γ ray. While some of the cross sections represent independent yields (labeled I in Table I), the majority are cumulative. The latter are identified as either $C+$ or $C-$ depending on whether they represent the integrated

isobaric cross section of more neutron-deficient or more neutron-excessive precursors, respectively. The cross sections of ^{22}Na and ^{24}Na were reduced by $\sim 5\%$ because of the direct production of these nuclides in Mylar. This effect is described in more detail in Sec. III C.

B. Parametrization of cross sections

Although we have measured a large number of cross sections, the data represent only a fraction of the total reaction cross section. In order to obtain the mass yield distribution, it is necessary to make estimates of the unmeasured cross sections. Rudstam[17] has proposed a semiempirical equation for the cross sections of spallation products. His six-parameter equation assumes that the mass-yield curve decreases exponentially with decreasing product mass number and that, at a given mass number, the isobaric yield distribution is Gaussian. We were unable to obtain an adequate fit with this expression because of the upturn in yields observed below $A \sim 30$ and the downturn in yields observed above $A \sim 60$. However, a 10-parameter expression previously used to fit the mass yield distribution obtained in the interaction of silver with relativistic heavy ions gave an excellent fit to the data.[18] The expression is

$$\sigma(Z, A) = \exp[\alpha_1 + \alpha_2 A + \alpha_3 A^2 + \alpha_4 A^3$$
$$+ (\alpha_5 + \alpha_6 A + \alpha_7 A^2) | Z_p - Z |^{\alpha_8}]. \quad (1)$$

The first four parameters, $\alpha_1 - \alpha_4$, determine the shape of the mass yield distribution, which is represented as an exponential in powers of A, with terms up to A^3. The parameters $\alpha_5 - \alpha_7$ determine the width of the isobaric yield distribution. The inclusion of the two A-dependent terms allows for a possible mass dependence in the width. The parameter α_8 determines the shape of the isobaric yield distribution at a given mass number, where $\alpha_8 = 2$ corresponds to a Gaussian distribution. Equation

TABLE I. Cross sections for the production of radionuclides in the interaction of copper with 35 MeV/nucleon ^{12}C ions.

Nuclide	Type	σ (mb)	Nuclide	Type	σ (mb)
^{22}Na	$C+$	1.76±0.19	^{52}Mn	I	26.0 ±2.2
^{24}Na	$C-$	1.43±0.17	^{52}Mn^m	$C+$	3.24±0.35
^{28}Mg	$C-$	0.10±0.02	^{52}Fe	$C+$	0.43±0.04
^{34}Cl^m	$C+$	0.21±0.02	^{54}Mn	I	69.3 ±7.0
^{39}Cl	$C-$	0.18±0.05	^{55}Co	$C+$	3.95±0.24
^{41}Ar	$C-$	0.35±0.04	^{56}Mn	$C-$	6.55±0.40
^{42}K	I	2.77±0.48	^{56}Co	$C+$	25.4 ±1.4
^{43}K	$C-$	0.83±0.55	^{57}Co	$C+$	86.0 ±6.6
^{44}Sc	I	2.45±0.25	^{57}Ni	$C+$	2.52±0.17
^{44}Sc^m	I	8.31±0.82	^{58}Co	I	93.9 ±7.9
^{46}Sc	I	10.1 ±0.5	^{59}Fe	$C-$	2.82±0.16
^{47}Sc	I	4.34±0.44	^{60}Co	I	21.2 ±2.7
^{48}Sc	I	0.49±0.08	^{60}Cu	$C+$	9.89±0.51
^{48}V	$C+$	22.5 ±1.3	^{61}Co	$C-$	3.70±0.22
^{48}Cr	$C+$	0.51±0.04	^{61}Cu	$C+$	43.1 ±4.2
^{49}Cr	$C+$	5.03±0.58	^{62}Zn	$C+$	6.02±0.58
^{51}Cr	$C+$	77.8 ±7.8	^{63}Zn	$C+$	20.7 ±1.1
			^{65}Zn	$C+$	36.1 ±3.6

(1) assumes that the isobaric yield distribution is symmetric about the most probable charge Z_p, which is assumed to vary with mass number as

$$Z_p = \alpha_9 A + \alpha_{10} A^2 . \tag{2}$$

The measured cross sections were fitted with Eq. (1) by means of an iterative least-squares code.[1] In the first iteration, Eq. (1) was fitted to both cumulative and independent yields. The cumulative cross sections were then corrected for isobaric feed-in by means of the calculated progenitor cross sections, and the resulting independent yields were refitted. This procedure converged after three iterations. Table II lists the values of the parameters $\alpha_1 - \alpha_{10}$.

The quality of the fit may be seen in a comparison of the data with the calculated isobaric-yield and mass yield distributions. In order to compare the independent yields derived from the measured cross sections with the isobaric yield distribution, it is convenient to divide both experimental and calculated cross sections by the calculated total isobaric cross section in order to obtain fractional isobaric yields, F. For display purposes, the experimental values of F are scaled to a common mass number, $A = 51$, using the ratio of calculated F values at $A = 51$ and at the mass number in question as the scaling factor. The results are shown in Fig. 1. Figure 2 shows a comparison of the measured cumulative cross sections, corrected for the missing yield at each mass number, with the fitted mass yield distribution. The uncertainties in the corrected data points include 20% uncertainties in the values of the unmeasured isotopic cross sections. Equations (1) and (2) provide a satisfactory representation of both the isobaric-yield and the mass yield distributions. In particular, our data do not require an asymmetric isobaric yield distribution, as apparently required by the data obtained at relativistic energies.[1]

C. Recoil properties

The results of the recoil measurements may be expressed in terms of the average forward range, FW, and the ratio of forward-to-backward emission, F/B. Here, F and B are the fractions of the total activity of a given nuclide collected in the forward and backward catchers,

TABLE II. Parameters obtained from the fit of Eq. (1) to the cross sections of $A = 22-65$ products from the interaction of copper with 35 MeV/nucleon ^{12}C ions.

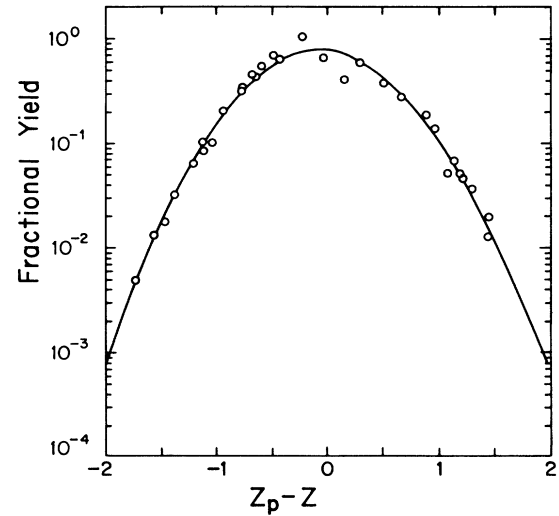| Parameter	Value
α_1	24.2 ± 0.2
α_2	-2.02 ± 0.02
α_3	$(5.27 \pm 0.04) \times 10^{-2}$
α_4	$-(4.10 \pm 0.04) \times 10^{-4}$
α_5	$-(4.56 \pm 1.10) \times 10^{-3}$
α_6	$-(8.14 \pm 0.49) \times 10^{-2}$
α_7	$(8.90 \pm 0.53) \times 10^{-4}$
α_8	1.93 ± 0.01
α_9	0.479 ± 0.000
α_{10}	$-(2.15 \pm 0.03) \times 10^{-4}$

FIG. 1. Fractional isobaric yield distribution for the interaction of copper with 35 MeV/nucleon ^{12}C ions. Curve, fitted values at $A = 51$; points, data scaled to $A = 51$.

respectively, and W is the target thickness. The results are listed in Table III. The tabulated uncertainties were determined in a similar manner as those in the cross sections.

The range of ^{24}Na was reduced by $\sim 5\%$ to correct for direct production in Mylar. As evidenced by the larger activity in the downstream as compared to the upstream guard foil, sodium nuclides produced in Mylar have a large enough forward range to transfer a significant fraction of the activity into the adjacent downstream foil. Consequently, the backward catcher foil required a sub-
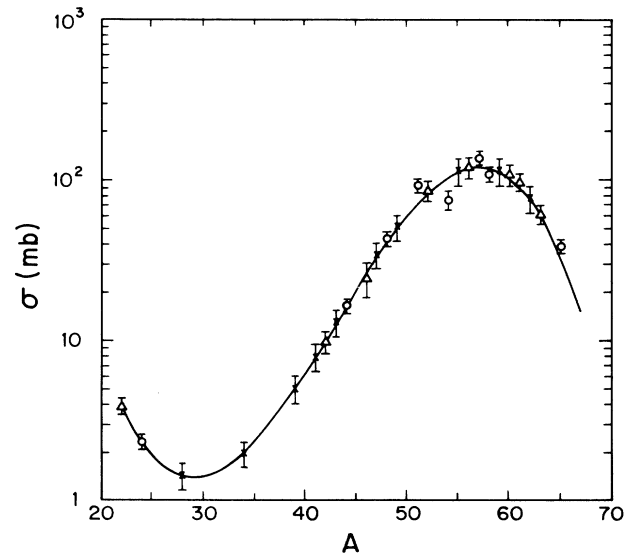

FIG. 2. Mass yield distribution for the interaction of copper with 35 MeV/nucleon ^{12}C ions. Curve, fit to data. Points, experimental values. The different symbols indicate the fraction of each yield that was measured: $\bigcirc$, $> 50\%$; $\triangle$, $20-50\%$; $\times$, $< 20\%$.

TABLE III. Recoil properties of products of the interaction of copper with 35 MeV/nucleon ^{12}C ions.

Nuclide	FW (mg/cm^2)	F/B	$v_\parallel/v_{CN}$[a]
^{24}Na	5.62±0.74	24.2±4.3	0.74±0.07
^{28}Mg	4.34±0.73	>47.1	1.06±0.18
^{42}K	2.53±0.38	94.8±22.1	0.69±0.09
^{43}K	2.46±0.30	83.9±31.0	0.66±0.08
^{44}Sc	2.43±0.26	>275	0.68±0.08
^{44}Sc^m	2.45±0.28	365±73	0.69±0.08
^{46}Sc	2.42±0.27	464±133	0.65±0.07
^{47}Sc	2.41±0.24	250±40	0.64±0.07
^{48}Sc	3.04±0.67	325±157	0.76±0.15
^{48}V	2.36±0.28	611±89	0.66±0.08
^{48}Cr	2.34±0.31	286±137	0.67±0.08
^{49}Cr	2.44±0.47	>19.9	0.68±0.12
^{51}Cr	2.28±0.28	331±92	0.62±0.07
^{52}Mn	2.45±0.27	1490±350	0.66±0.07
^{52}Fe	2.23±0.34	456±369	0.63±0.09
^{54}Mn	2.17±0.27	>696	0.58±0.07
^{55}Co	2.12±0.27	>300	0.59±0.07
^{56}Mn	2.23±0.31	171±59	0.58±0.07
^{56}Co	1.93±0.21	455±80	0.54±0.05
^{57}Co	1.77±0.20	539±143	0.50±0.05
^{57}Ni	1.83±0.24	128±59	0.52±0.07
^{58}Co	1.61±0.16	171±81	0.46±0.06
^{59}Fe	1.34±0.20	94.9±53.2	0.39±0.06
^{60}Co	1.15±0.27	>135	0.35±0.08
^{61}Co	0.85±0.10	35.2±21.4	0.29±0.03
^{61}Cu	1.09±0.13	>17.9	0.35±0.04
^{62}Zn	1.06±0.15	114±92	0.34±0.04
^{65}Zn	1.09±0.13	95.6±54.5	0.34±0.04

[a]The velocity of the compound nucleus is 1.296 (MeV/u)$^{1/2}$.

stantial correction for Na recoils from the adjacent upstream guard foil. Thus, the F/B ratio of ^{24}Na was increased by $\sim 100\%$. The target foil activity similarly includes a small contribution of Na recoils originating in the backward catcher. The correction to the cross section took into account the extraneous Na activity in both target and catchers. The sodium isotopes were the only nuclides that required a correction for activation effects in the Mylar.

The variation of the forward ranges and F/B ratios with product mass number is displayed in Figs. 3 and 4, respectively. The ranges vary inversely with mass number, with the increase in range for the lightest products being particularly noticeable. With the exception of ^{24}Na, the F/B ratios are very large, typically over 100. This result is a qualitative indication of substantial momentum transfer.

IV. DISCUSSION

A. Isobaric yield distribution

The isobaric yield distribution, Fig. 1, is near-Gaussian in shape. The shape parameter $\alpha_8 = 1.93$ ±0.01, indicating that the curve has slightly broader wings than a Gaussian. The dependence of the isobaric
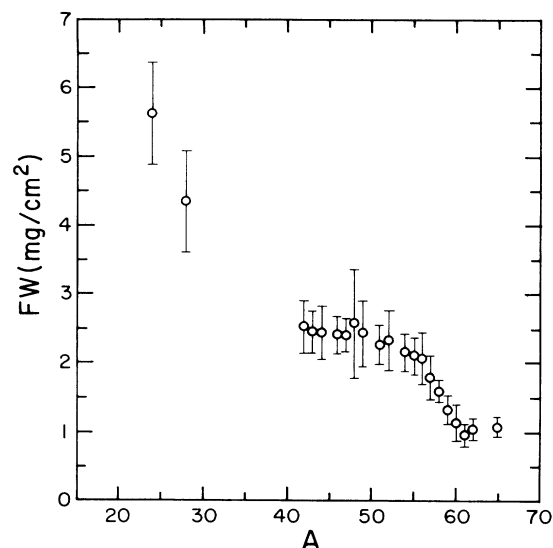

FIG. 3. Dependence of the mean forward ranges FW on product mass number.

yield distribution on mass number can be seen in plots of Z_p and the full width at half maximum versus A, as shown in Fig. 5. The mass dependence of Z_A, the most stable charge at A, is also shown. We see that the most probable yields of light products occur for nuclides very close to stability, while those of the heavier products are found for neutron deficient nuclides. The width of the isobaric yield distribution is fairly insensitive to mass number.

The results may be compared with other relevant measurements of the interaction of copper with intermediate-energy projectiles. Orth et al.[19] have measured the yields of products of the interaction of copper with 350 MeV protons, which have nearly the same total kinetic energy as the ^{12}C ions used in the present work. Lund et al.[10] have performed similar measurements with
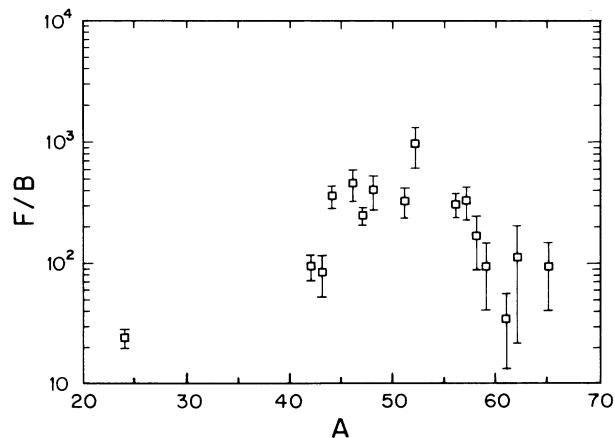

FIG. 4. Dependence of forward-backward ratios F/B on product mass number.

86 MeV/nucleon ^{12}C ions. We have used the procedure described in Sec. III B to obtain the isobaric-yield and mass yield distributions from the reported cross sections. The resulting values of Z_p/A and width of the isobaric yield distribution are included in Fig. 5.

The values of Z_p are virtually independent of projectile identity or energy in the regime of interest. The widths of the previously reported distributions have a comparable sensitivity to mass number as the present widths but are somewhat larger in magnitude. The value of the parameter α_8, which determines the shape of the distribution, is 2.27±0.02 for 350 MeV protons and 2.57±0.02 for 86 MeV/nucleon ^{12}C ions. A value of $\alpha_8 > 2$ indicates that the curve drops off more steeply than a Gaussian in the region of the wings. This effect counteracts that of the larger widths—all three isobaric yield distributions are, in actuality, very similar. We conclude that the isobaric yield distributions are independent of projectile identity and energy for the limited range of energies and particle types covered by this comparison. This has been taken as an indication of the dominance of the deexcitation phase of the reaction.[20]

B. Mass yield distribution

The mass yield distribution, Fig. 2, goes through a maximum at $A \sim 58$, decreases to a minimum at $A \sim 30$, with the decrease being exponential over much of this interval, and then increases at lower mass numbers. With the exception of ^{65}Zn, we did not observe any significant yields of trans-target products.

Figure 6 shows a comparison of the present mass yield curve with those derived from the 86 MeV/nucleon ^{12}C and the 350 MeV proton data.[10,19] The mass yield curves based on the ^{12}C experiments have a similar overall shape, although a number of differences in detail may be noted. Thus, the average mass of the products formed at 86 MeV/nucleon, 51.1 u, is about 4 u smaller than that obtained at 35 MeV/nucleon, 55.2 u. Furthermore, the dropoff of yields in the exponential region is steeper at the lower energy. Finally, the yields of low-mass products are higher at the higher energy. However, the minimum at $A \sim 30$ is more pronounced at the lower energy. These differences indicate that higher excitation energies are available at the higher bombarding energy, leading to larger mass losses and flatter mass yield distributions.

The mass yield curve derived from the 350 MeV proton data shows that the total spallation cross section for protons is less than half as large as that for 35 MeV/nucleon ^{12}C ions. However, the mean mass loss over the common mass range is nearly comparable, being some 2–3 u larger for ^{12}C ions than for protons. Since the proton kinetic energy is 50 MeV less than the total ^{12}C kinetic energy, the actual difference at the same total kinetic energy is presumably even smaller. Thus, it appears that the mean excitation energy transferred in the interaction of an intermediate energy projectile to a struck nucleus depends on the projectile energy but is nearly independent of its mass.
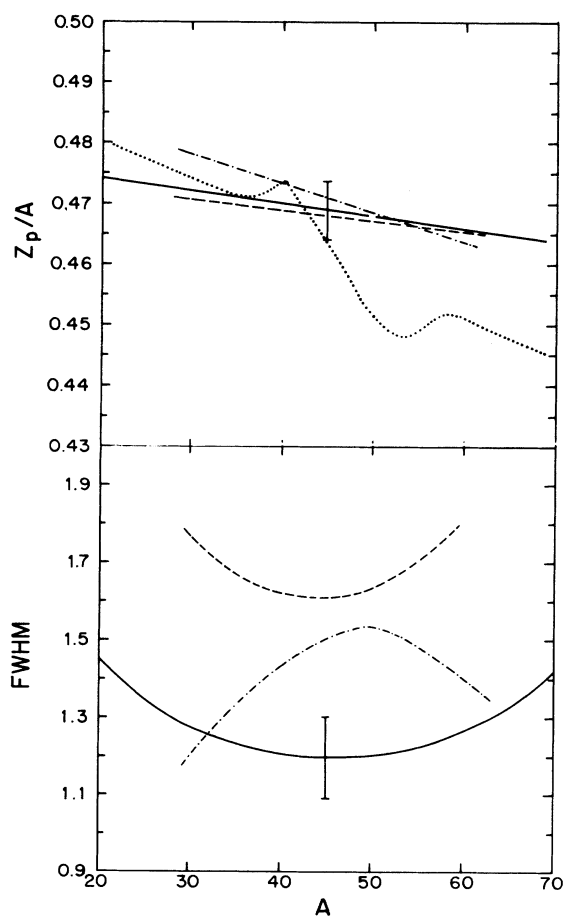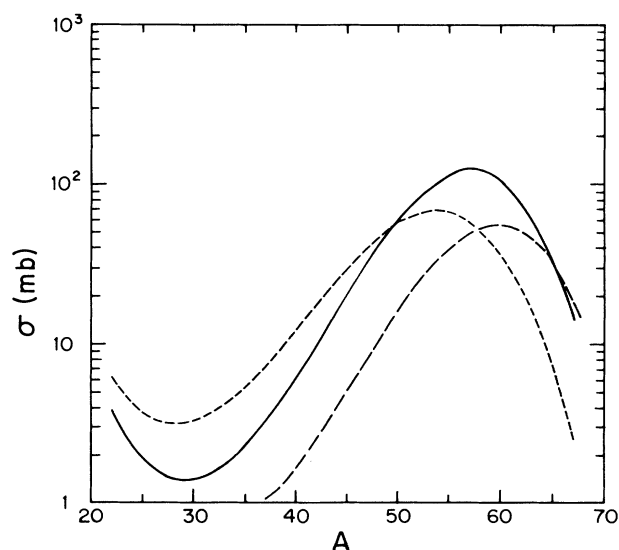

FIG. 5. Mass dependence of Z_p/A (top panel) and of the full width at half maximum of the isobaric yield distribution (bottom). Typical error bars are shown. The dotted curve shows the variation of Z_A/A. The dashed curves show the results derived from 86 MeV/nucleon data (Ref. 10) and the dot-dashed curves those derived from 350 MeV p data (Ref. 19).

FIG. 6. Comparison of the mass yield distribution for the interaction of copper with 35 MeV/nucleon ^{12}C ions (solid curve), 86 MeV/nucleon ^{12}C ions (Ref. 10, dashed curve), and 350 MeV p (Ref. 19, long dashes).

Cumming *et al.*[3] have noted that the slope of the mass yield curve in the region of the exponential dropoff increases with decreasing projectile kinetic energy and is an approximate measure of the mean excitation energy transferred to the struck nucleus in the initial interaction. The present mass yield curve does not vary exponentially over the same mass region as the higher energy data of Cumming *et al.*[3] Nonetheless, in order to make possible a comparison with the higher energy results, we have fitted the region between $A = 37$ and 57 with an exponential. The slope is 19% per mass number. This value agrees approximately with the Cumming systematics, which are based on reactions induced by protons and α particles in this energy regime. This agreement is yet another indication that the excitation energy transfer depends on the projectile kinetic energy but is virtually independent of its identity in this energy regime.

C. Total reaction cross section

We can obtain an estimate of the total reaction cross section σ_R by integrating the mass yield distribution. The value obtained by integration between $A = 28$ and 68 is 1.72 ± 0.26 b. The fitted curve was extrapolated to $A = 68$, thereby adding ~ 20 mb to σ_R, in order to account for any unobserved trans-target products. The cutoff at $A = 28$ obviously does not take into account the upturn in yields observed at lower mass numbers. However, recent experiments indicate that, at the projectile energies of present interest, light fragments are formed primarily in a binary process in which the two fragments share virtually all of the available mass.[21] Consequently, fragments with $A < 28$ should have partners whose yield has been included in our integration procedure.

There have been several reported measurements of total reaction cross sections for intermediate-energy heavy ions. Two of these are especially pertinent to the present work. Sahn *et al.*[22] measured the elastic scattering angular distributions of 35 MeV/nucleon ^{12}C ions on nuclear targets and derived values of σ_R by means of an optical model analysis. An interpolation between their values for ^{40}Ca and ^{90}Zr, performed on the assumption of a linear variation with $(A_{proj}^{1/3} + A_{targ}^{1/3})^2$, gives a value for copper of 2.26 ± 0.23 b. Kox *et al.*[23] performed a direct attenuation measurement of σ_R for 30 MeV/nucleon ^{12}C ions and various nuclear targets. The results for ^{64}Zn are $\sigma_R = 2.43 \pm 0.17$ b. These workers also give a new parametrization of σ_R which, for the conditions of our experiment, gives $\sigma_R = 2.46$ b for copper plus ^{12}C.

The present value of σ_R (1.72 ± 0.26 b) is significantly lower than the other reported values. The discrepancy might indicate that interactions in which the target breaks up into two or more fragments, none of which have $A \geq 27$, could occur at the 10–20% level. In addition, the occurrence of interactions populating very specific final states to a much larger extent than predicted by the cross-section parametrization, e.g., excited states of the target nucleus, would not have been detected in our study.

D. Comparison with calculations

Mass-yield and isobaric yield distributions have traditionally been compared with cascade-evaporation calculations. Thus, we first compared our results with the code ISABELLE, designed to simulate the interaction of energetic heavy ions with nuclei.[24] However, we found the code to be inapplicable at these low energies, which, in actuality, are outside reasonable application of the assumptions of the model. However, the evaporation part of the calculation, i.e., the code EVA,[25] is presumably applicable. We have simulated the primary cascade by a simple approximation consistent with the experimental data and then used the statistical code EVA to simulate the deexcitation.

As discussed in Sec. IV E, the longitudinal momentum transfer ranges from approximately 30–80 % of the projectile momentum, depending on product mass. Such momentum transfers can be achieved by incomplete fusion. We have calculated the final mass yield distribution on the assumption that a ^{4}He, ^{6}Li, ^{9}Be, or ^{12}C moving with beam velocity is captured by the target in the initial interaction. The resulting mass yield distributions are shown in Fig. 7, where the curves have been normalized to our experimental value of σ_R. We note that the calculated peak in the mass yield curve moves to lower masses and the distribution broadens as the mass of the fragment captured by the target increases. This trend is caused by the fact that the energy per nucleon of the projectile is substantially larger than the energy required to evaporate a nucleon. Thus, more nucleons will be evaporated for each additional transferred nucleon.

The overall calculated mass yield distribution, obtained by averaging the individual curves, is also shown.
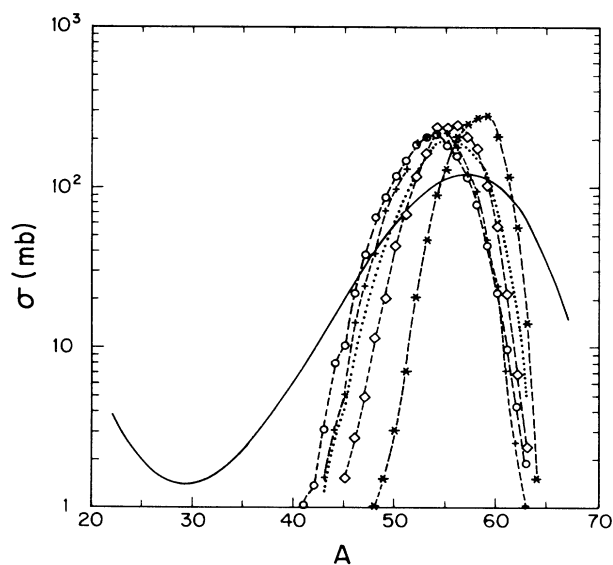

FIG. 7. Comparison of the experimental mass yield distribution (solid curve) with the evaporation code EVA (Ref. 25). The different calculations correspond to a composite nucleus consisting of the target plus a transferred projectile fragment consisting of an α particle ($*$), ^{6}Li ($\Diamond$), ^{9}Be ($+$), and ^{12}C ($\circ$). The dotted curve represents the average of the individual calculated curves.

Although the calculation predicts the approximate position of the peak in the distribution, it does not predict a sufficiently broad curve and severely underestimates the yields of fragments below $A \sim 40$. While the calculation cannot, of course, predict the occurrence of processes responsible for the upturn in the yields of low-mass products, the discrepancy is already present in the region of exponentially decreasing cross sections, where spallation presumably still is the dominant mechanism.

In order to determine the sensitivity of the results to the particular model used to simulate the deexcitation, the calculation was also performed by means of the code ALICE, based on the geometry dependent hybrid preequilibrium model.[26] This code should provide a more realistic description than EVA because it incorporates angular momentum effects as well as preequilibrium emission. Since the model does not consider the initial heavy ion-nucleus interaction, we made the same assumptions concerning incomplete fusion as described above. The results are shown in Fig. 8. The predicted curves resemble those obtained by means of the code EVA and lend credence to the notion that the formation of products with $A \lesssim 40$ cannot be described as resulting from the evaporation of nucleons and complex particles up to α particles, the heaviest evaporated particles included in either code.

Figure 9 shows a comparison of the isobaric yield distributions obtained at $A = 51$ from ALICE and EVA with the scaled experimental data (Fig. 1). The distribution predicted by EVA is slightly broader than the experimental curve but peaks at the same point. Evidently, the isobaric yield distribution is less sensitive to the details of the excitation energy spectrum of the composite system then the mass yield distribution. The isobaric yield distribution obtained from ALICE is somewhat less satisfactory since it is shifted by nearly one Z unit to the neutron deficient side.
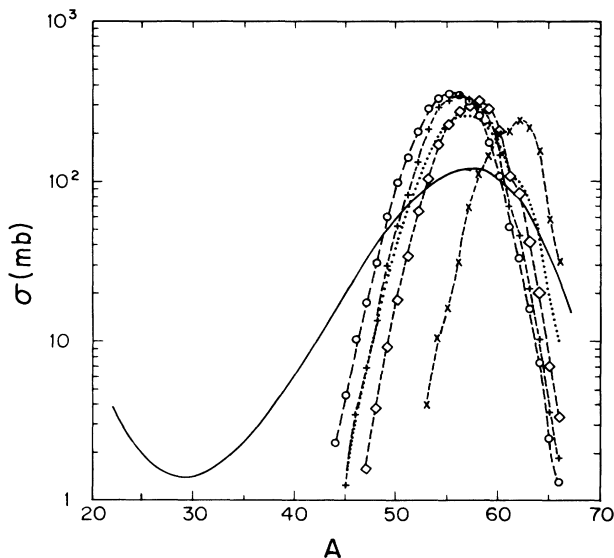

FIG. 8. Comparison of the experimental mass yield distribution with the preequilibrium code ALICE (Ref. 26). The various curves have the same meaning as in Fig. 7.
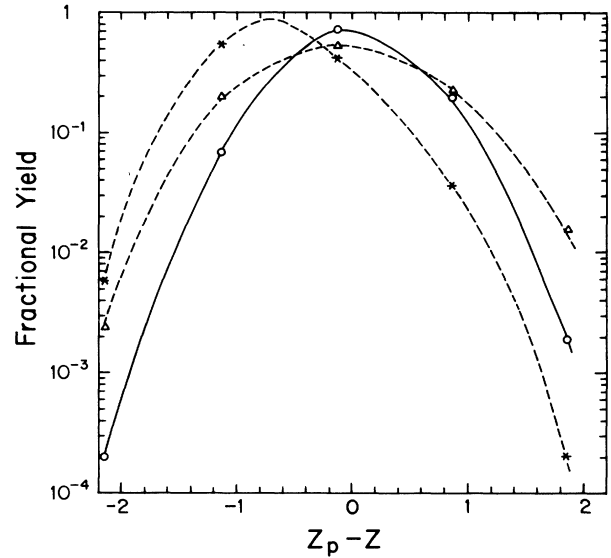

FIG. 9. Comparison of the isobaric yield distribution scaled to $A = 51$ (○) with the distributions obtained at this mass number with the codes EVA (△) and ALICE (∗).

E. Longitudinal momentum transfer

Longitudinal momentum transfer (LMT) measurements in intermediate energy reactions are a subject of current interest because of the information they convey about the reaction mechanism. The systematics of LMT show that complete fusion gives way to incomplete fusion when the projectile energy exceeds 8–10 MeV/nucleon. Furthermore, when expressed as a fraction of the projectile momentum, the LMT decreases nearly linearly with relative projectile velocity and is approximately independent of target mass or projectile identity.[27–29] It also appears that the LMT saturates at approximately 180 MeV/c per incident nucleon.[29,30] The present results permit us to explore another aspect of the LMT, namely its variation with product mass. The relationship between LMT and excitation energy allows us to examine some features of the excitation energy deposited in the composite system.

The most common method of extracting LMT values from thick target–thick catcher recoil measurements is to use relationships based on the two-step model.[31] On the basis of certain simplifying assumptions, the experimental range $2W(F+B)$ and the F/B ratio are used to obtain the longitudinal velocity $v_{\parallel}$ imparted to the composite system in the initial interaction and the velocity V acquired by the observed product in the deexcitation step. The most refined formulation has been given by Winsberg.[32] However, solutions to the equations relating $v_{\parallel}$ and V to the experimental quantities can only be obtained on the basis of approximations that neglect higher order terms in the quantity $\eta = v_{\parallel}/V$. The very large values of F/B observed for most products indicate that $\eta > 1$. Thus, the neglect of higher order terms is not justified.

A second method for obtaining LMT values from

recoil data has been proposed by Cumming *et al.*[5,12] In this procedure, trial values of $v_\parallel$ and V are assumed and used to infer values of FW and F/B. The values of $v_\parallel$ and V that lead to optimum agreement with experiment are adopted.

Winsberg and Alexander[33] have shown that the evaporation velocity V has a negligible effect on thick-target recoil properties in reactions for which $\eta^{-1} < 1$, i.e., heavy ion reactions involving substantial LMT. The neglect of V becomes an increasingly valid approximation as η^{-1} decreases and as the regime in which recoil range is proportional to recoil velocity is approached. If the effect of V is neglected, the velocity corresponding to FW is just $v_\parallel$.

We have obtained $v_\parallel$ values from the data on the basis of all the above approaches. In performing these calculations we used the range-energy tables of Northcliffe and Schilling[34] after first converting the tabulated path lengths to projected ranges by means of the LSS formalism.[35] We found that for most products the values of $v_\parallel$ obtained by the method of Winsberg and Alexander[33] were in excellent agreement with those obtained by Cumming.[12] However, the approach proposed by Winsberg[32] gave $v_\parallel$ values that were some 20% lower. The values of $v_\parallel/v_{CN}$ (CN denotes compound nucleus) tabulated in Table III were obtained following the approach of Winsberg and Alexander.[33] The nuclide ^{24}Na is exceptional. The large range and relatively low F/B value obtained for this product indicate that its recoil properties are determined by both V and $v_\parallel$. The listed value was therefore obtained by means of the Winsberg method.

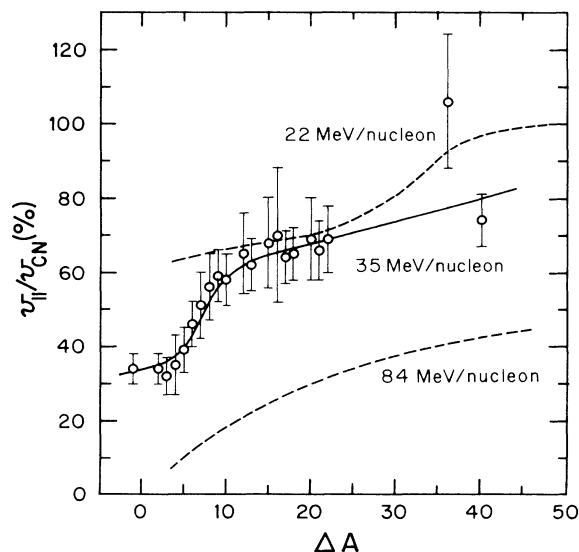The $v_\parallel/v_{CN}$ values associated with the formation of

FIG. 10. Variation with mass loss ΔA of the fractional velocity transfer in the interaction of copper with ^{12}C ions. The solid curve through the points shows the trends in the present data. Smooth curves drawn through the values obtained at 22 and 84 MeV/nucleon (Ref. 12) are included. The velocity is expressed in terms of that of the putative compound nucleus. The mass loss is given relative to the target mass.

products of mass A are plotted versus mass loss from the target in Fig. 10. The velocities increase with the mass loss, ranging from $\sim 30\%$ of the compound nucleus value for products close to the target to $\sim 80\%$ for the lighter products. This behavior can be understood in view of the proportionality between the fractional momentum transfer and the fractional excitation energy transfer to the struck nucleus.[36] Since the mass loss is, to first order, proportional to the excitation energy, the observed trend follows.

Fractional momentum transfer in the interaction of copper with intermediate energy ^{12}C ions has been determined previously at 84 and 22 MeV/nucleon.[12] Figure 10 includes the results obtained at these energies. A gradual increase in fractional momentum transfer with decreasing projectile energy may be noted. This trend is expected from the systematics of the LMT variation with projectile energy.[27-29] However, the observed variation of the LMT with mass loss indicates that care must be taken in drawing conclusions from systematics based on LMT values averaged over all interactions.

The average value of the fractional LMT obtained from our data by weighting the experimental values by the mass yield distribution is 0.53 ± 0.04, corresponding to an LMT of 1.6 ± 0.1 GeV/c. The LMT systematics[27-29] predicts a fractional LMT of 0.6–0.7 at the relative velocity appropriate to our experiment. While the predicted value is significantly larger than our result, a recent calculation of the fractional LMT based on a leading particle collision model predicts a significant increase in LMT with target mass.[37] Since copper lies at the low mass end of the targets which form the basis of the LMT systematics, the discrepancy is probably not significant.

The values of $v_\parallel$ can be interpreted in terms of a commonly used model, which pictures the initial interaction as involving incomplete fusion, with beam velocity particles of total mass Δm escaping at $0°$. The values of Δm range from approximately 8 for products close to the target to 3 for the lightest products, the average value being ~ 6. This trend is suggestive of a geometric origin, with products close to the target formed in peripheral interactions and those of low mass formed in more central collisions. The abrasion-ablation model of relativistic heavy ion interactions[38] predicts just such a trend in Δm values. Thus, certain features of this model must be already valid at the relatively low energies of present interest.

The excitation energy of the composite nucleus can be obtained on the basis of the same assumptions used to obtain the values of Δm. Following Leray,[29] we assume in the estimation of the Q values for the formation of the composite systems that the missing mass Δm is emitted as free nucleons. The excitation energy is plotted versus mass loss ΔA in Fig. 11(a). As expected from Fig. 10, the excitation energy increases with the mass loss, ranging from ~ 70 to 300 MeV. The composite system is formed with temperatures in the 3–6 MeV range.

The formation of spallation products involves the dissipation of the excitation energy of the composite system via nucleon and light particle evaporation. Figure 11(b)
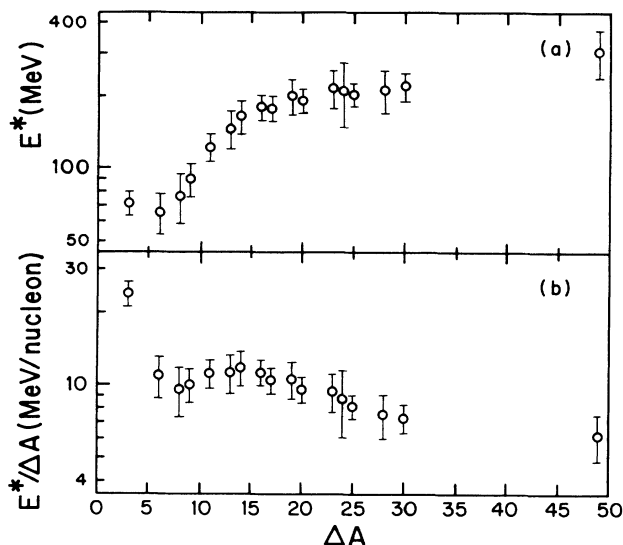
FIG. 11. Variation with mass loss ΔA of (a) the mean excitation energy and (b) the mean excitation energy per unit mass loss associated with the formation of products of the interaction of copper with 35 MeV/nucleon ^{12}C ions. The mass loss is expressed relative to the mass of the composite system, which is determined by means of an approximation discussed in the text.

shows a plot of the excitation energy per unit mass loss. Over much of the product mass range the values of $E^*/\Delta A$ are in the vicinity of 10 MeV/nucleon. This is a reasonable value for a process in which the mass is removed chiefly by nucleon evaporation. However, the formation of the lightest products involves $E^*/\Delta A$ values of only ~6 MeV/nucleon. This result indicates that complex aggregates, which generally have much lower separation energies per nucleon than do nucleons, must be emitted in the formation of these products. The kinetic energy of ^{24}Na (in the moving system) is close to the tangent spheres value for binary breakup, providing further evidence that this product is not formed by spallation. The upturn in the mass yield distribution ob-

served in the low product mass region provides another indication of such a change in mechanism.

V. CONCLUSIONS

The interaction of copper with 35 MeV/nucleon ^{12}C ions has been studied. The isobaric yield distribution is near-Gaussian; the most probable yields occur very close to stability for products below $A \sim 45$, but occur on the neutron deficient side of stability at higher mass numbers.

The mass yield distribution peaks at $A \sim 58$, decreases to a minimum at $A \sim 30$, and increases again at lower mass numbers. The only trans-target product observed was ^{65}Zn. Both the isobaric-yield and mass yield distributions have been compared with the results of other intermediate-energy measurements. To first order, both distributions are independent of projectile mass in this regime. While the isobaric yield distribution is also independent of energy, the mass yield distribution shifts to lower masses with increasing energy. The results have been compared with both evaporation and preequilibrium model calculations on the assumption that the initial interaction involves incomplete fusion. Neither model can satisfactorily account for all the results.

The total reaction cross section was obtained by integration of the mass yield distribution as 1.72 ± 0.26 b, which is a significantly lower value than those given by other experiments. Possible reasons for the discrepancy have been discussed.

The average longitudinal momentum transfer in the interaction corresponds to $53 \pm 4\%$ of the projectile momentum, i.e., to 1.6 ± 0.1 GeV/c. The momentum transfer increases with decreasing product mass and ranges from about 30% to 80% of the projectile momentum. The corresponding excitation energies of the composite system range from approximately 70 to 300 MeV.

*Present address: Department of Chemistry, Hallym University, Chooncheon, Korea 200.

[1]J. B. Cumming, P. E. Haustein, R. W. Stoenner, L. Mausner, and R. A. Naumann, Phys. Rev. C **10**, 739 (1974).

[2]J. B. Cumming, R. W. Stoenner, and P. E. Haustein, Phys. Rev. C **14**, 1554 (1976).

[3]J. B. Cumming, P. E. Haustein, T. J. Ruth, and G. J. Virtes, Phys. Rev. C **17**, 1632 (1978).

[4]J. B. Cumming, P. E. Haustein, and H. C. Hseuh, Phys. Rev. C **18**, 1372 (1978).

[5]J. B. Cumming, P. E. Haustein, and H. C. Hseuh, Phys. Rev. C **24**, 2162 (1981).

[6]K. H. Hicks et al., Phys. Rev. C **26**, 2016 (1982).

[7]G. D. Cole and N. T. Porile, Phys. Rev. C **24**, 2038 (1981).

[8]G. D. Cole and N. T. Porile, Phys. Rev. C **25**, 244 (1982).

[9]T. Lund et al., Phys. Lett. **102B**, 239 (1981).

[10]T. Lund et al., Z. Phys. A **306**, 43 (1982).

[11]A. Lleres, J. Blachot, J. Crancon, A. Gizon, and H. Nifenecker, Z. Phys. A **312**, 177 (1983).

[12]L. Kowalski, P. E. Haustein, and J. B. Cumming, Phys. Rev. Lett. **51**, 642 (1983).

[13]F. Hubert, A. Fleury, R. Bimbot, and D. Gardes, Ann. Phys. (Paris) **5**, 1 (1980).

[14]T. Routti and S. G. Prussin, Nucl. Instrum. Methods **72**, 125

(1969).

[15]J. B. Cumming, National Academy of Sciences Report NAS-NS-3107, 1962, p. 25 (unpublished).

[16]U. Reus and W. Westmeier, At. Data Nucl. Data Tables **29**, 2 (1983).

[17]G. Rudstam, Z. Naturforsch. **219**, 1027 (1966).

[18]N. T. Porile, G. D. Cole, and C. R. Rudy, Phys. Rev. C **19**, 2288 (1979).

[19]C. J. Orth, B. J. Dropesky, R. A. Williams, G. C. Giesler, and J. Hudis, Phys. Rev. C **18**, 1426 (1978).

[20]D. J. Morrissey et al., Phys. Rev. Lett. **43**, 1139 (1979).

[21]R. J. Charity et al., Phys. Rev. Lett. **56**, 1354 (1986).

[22]C. C. Sahn et al.,, Phys. Rev. C **34**, 2165 (1986).

[23]S. Kox et al., Phys. Rev. C **35**, 1678 (1987).

[24]Y. Yariv and Z. Fraenkel, Phys. Rev. C **20**, 2227 (1979).

[25]I. Dostrovsky, Z. Fraenkel, and G. Friedlander, Phys. Rev. **116**, 683 (1959).

[26]M. Blann, Nucl. Phys. **A213**, 570 (1973).

[27]V. Viola et al., Phys. Rev. C **26**, 178 (1982).

[28]Y. Chan et al., Phys. Rev. C **27**, 447 (1983).

[29]S. Leray, J. Phys. C **4**, 275 (1986).

[30]J. Galin et al., Phys. Rev. Lett. **48**, 1787 (1982).

[31]N. Sugarman, M. Campos, and K. Wielgoz, Phys. Rev. **101**, 388 (1956).

[32]L. W. Winsberg, Nucl. Instrum. Methods **150**, 465 (1978).

[33]L. Winsberg and J. M. Alexander, Phys. Rev. **121**, 518 (1961).

[34]L. C. Northcliffe and R. F. Schilling, Nucl. Data Tables **A7**, 233 (1970).

[35]J. Lindhard, M. Scharff, and H. E. Schiott, K. Dansk. Vidensk. Selsk. Mat.-Fys. Medd. **33**, No. 14 (1963).

[36]N. T. Porile, Phys. Rev. **120**, 572 (1960).

[37]J. B. Natowitz et al., Z. Phys. A **325**, 467 (1986).

[38]J. D. Bowman, W. J. Swiatecki, and C. F. Tsang, Lawrence Berkeley Laboratory Report No. LBL-2908, 1973 (unpublished).